Specific Localization of Serine 19 Phosphorylated Myosin II during Cell Locomotion and Mitosis of Cultured Cells

Fumio Matsumura, Shoichiro Ono, Yoshihiko Yamakita, Go Totsukawa, and Shigeko Yamashiro

Department of Molecular Biology and Biochemistry, Rutgers University, Nelson Labs, Busch Campus, Piscataway, New Jersey 08855

Abstract. Phosphorylation of the regulatory light chain of myosin II (RMLC) at Serine 19 by a specific enzyme, MLC kinase, is believed to control the contractility of actomyosin in smooth muscle and vertebrate nonmuscle cells. To examine how such phosphorylation is regulated in space and time within cells during coordinated cell movements, including cell locomotion and cell division, we generated a phosphorylation-specific antibody.

Motile fibroblasts with a polarized cell shape exhibit a bimodal distribution of phosphorylated myosin along the direction of cell movement. The level of myosin phosphorylation is high in an anterior region near membrane ruffles, as well as in a posterior region containing the nucleus, suggesting that the contractility of both ends is involved in cell locomotion. Phosphorylated myosin is also concentrated in cortical microfilament bundles, indicating that cortical filaments are under tension. The enrichment of phosphorylated myosin in the moving edge is shared with an epithelial cell sheet; peripheral microfilament bundles at the leading edge contain a higher level of phosphorylated myosin. On the other hand, the phosphorylation level of circumferential microfilament bundles in cell–cell contacts is low. These observations suggest that peripheral microfilaments at the edge are involved in force production to drive the cell margin forward while microfilaments in cell–cell contacts play a structural role. During cell division, both fibroblastic and epithelial cells exhibit an increased level of myosin phosphorylation upon cytokinesis, which is consistent with our previous biochemical study (Yamakita, Y., S. Yamashiro, and F. Matsumura. 1994. *J. Cell Biol.* 124:129–137). In the case of the NRK epithelial cells, phosphorylated myosin first appears in the midzones of the separating chromosomes during late anaphase, but apparently before the formation of cleavage furrows, suggesting that phosphorylation of RMLC is an initial signal for cytokinesis.

Myosin II is one of the best characterized of the major motor proteins of animal cells. This "conventional myosin" is involved in a variety of processes including muscle contraction, cell locomotion, cell division, and receptor capping (14, 29). In smooth muscle and vertebrate nonmuscle cells, myosin light chain kinase (MLCK)[1]-mediated phosphorylation of the regulatory light chain of myosin II (RMLC) at Serine 19 (S19) is believed to promote the contractility and stability of actomyosin (28, 30).

Address all correspondence to F. Matsumura, Department of Molecular Biology and Biochemistry, Rutgers University, Nelson Labs, Busch Campus, Piscataway, NJ 08855. Tel.: (732) 445-2838. (732) 445-4213. E-mail: Matsumura@mbcl.rutgers.edu

S. Ono's present address is Department of Pathology, Emory University, Woodruff Memorial Building, 7007A, Atlanta, GA 30322.

1. *Abbreviations used in this paper*: MLCK, myosin light chain kinase; PVDF, polyvinylidene difluoride; RMLC, regulatory myosin light chain; S19, serine 19.

In an in vitro system, S19 phosphorylation of RMLC results in a marked increase in both the stability of myosin filaments and the activity of actin-activated myosin Mg-ATPase. Other biochemical analyses have revealed that the level of phosphorylation of nonmuscle RMLC increases concomitantly with the massive contraction of nonmuscle cells after stimulation with serum or certain drugs (10, 11, 19), as well as during cytokinesis (33), suggesting that myosin phosphorylation plays an important role in the contraction and motility in vivo. On the other hand, the mutational analyses using *Dictyostelium discoideum* myosin II showed that neither phosphorylation of myosin light chain nor the binding of myosin light chain to heavy chain seems to be required for cell motility and cytokinesis of this organism (23, 31, 35). Perhaps the regulatory mechanism in this organism could be very different from that of higher eukaryotes, as myosin heavy chain phosphorylation appears to be more important for the regulation of cell motility in *Dictyostelium* (7, 12).

Our understanding of the role of the S19 phosphoryla-

tion in controlling the motility of cells and subcellular structures is limited by a lack of information regarding how such phosphorylation is regulated within cells in space and time. Biochemical analyses can not provide the spatial and temporal resolution needed to examine the role of S19 phosphorylation in cell division, nonmuscle cell locomotion, and other complex motile events. An indication of the subtle level of regulation involved is the observation that contraction and relaxation occur simultaneously in different parts of single motile cells. Contractile events during cytokinesis may be even more precisely controlled, as the precision of both the localization and timing of such events would appear to be critical to a successful outcome.

One way to examine the localization of phosphorylated RMLC is to generate a phosphorylation specific antibody (3, 26). Although such studies have demonstrated the localization of phosphorylated myosin in smooth muscle (3), localization in nonmuscle cells has not been reported. Taylor and his coworkers (see reference 6) have recently developed a new means to examine the dynamic behavior of phosphorylated myosin using a fluorescent protein biosensor of RMLC, which uses the phosphorylation-dependent changes in a ratio of fluorescence energy transfer. Their studies have shown that in motile fibroblasts, phosphorylated myosin is highest in the tail and lowest near the leading edge, and that dividing cells show temporal and spatial regulation of myosin phosphorylation (6, 25). Whereas the above study has generated important information, an independent approach should be made to understand the role of RMLC phosphorylation. We have developed a new S19 phosphorylation-specific anti–myosin II antibody, and used this reagent to examine the spatial and temporal regulation of RMLC phosphorylation at S19. We show that S19 phosphorylation is regulated in distinct patterns within motile and dividing fibroblastic and epithelial cells. The observed distribution patterns are consistent with a role for this phosphorylation event in triggering contraction associated with cell locomotion, wound closure, and cytokinesis.

Materials and Methods

Preparation of Antibody Against S19-phosphorylated RMLC

A phosphopeptide (R-P-Q-R-A-T-z-N-V-F-A-C; z = phosphoserine) corresponding to S19-phosphorylated RMLC was commercially synthesized by Chiron (St. Louis, MO), and 5 mg of the phosphopeptide was conjugated to 31 mg of a carrier protein, diphtheria toxoid by the same company. The conjugated peptide was freeze dried and dissolved in 5 ml in 0.1 M phosphate buffer, pH 7.0. Two rabbits were immunized with 1/40 of the conjugated peptide emulsified in Freund's complete adjuvant, and boosted every 4 wk with the same antigen solution emulsified in Freund's incomplete adjuvant. Serum from one rabbit showed a reaction to RMLC phosphorylated by MLCK and was further boosted for over 1 yr. Immunoglobulin G was precipitated by 50% saturated ammonium sulfate, and purified by protein A–Sepharose chromatography. The antibody (called pp2b) was affinity purified with a phosphorylated RMLC–Sepharose column, and absorbed with a dephosphorylated RMLC–Sepharose column.

Preparation of Total Cell Lysates and Immunoblotting

Total cell lysates were prepared as follows. Normal rat kidney cells (NRK, ATCC CRL-1571, and epithelial type) were quickly washed with PBS, and homogenized in PBS via several passages through a 25-gauge needle. The homogenates were then split and half was mixed with an equal volume of 2× SDS sample buffer. To the other half, MLCK, calmodulin, ATP, and $CaCl_2$ were added to the final concentrations of 4 μg/ml, 1 μg/ml, 2 mM, and 0.1 mM, respectively. After incubation for 15 min at room temperature, an equal volume of 2× SDS sample buffer was added. Both samples were homogenized, separated on SDS gels, and then blotted on polyvinylidene difluoride (PVDF) membranes.

For immunoblotting, PVDF membranes were incubated with 4 μg/ml of affinity-purified pp2b antibody in the presence of 0.1 mg/ml of BSA, and immunoreaction was detected with peroxidase-conjugated second antibody using a chemiluminescence method (Amersham Corp., Arlington Heights, IL).

Urea/Glycerol Gel Electrophoresis

Urea/glycerol gel electrophoresis was performed as described (24). Gels were soaked for 10 min in the SDS gel running buffer containing 25 mM Tris-glycine, pH 8.3, and 0.1% SDS, transferred to a nitrocellulose membrane, and then immunoblotted with pp2b as described above.

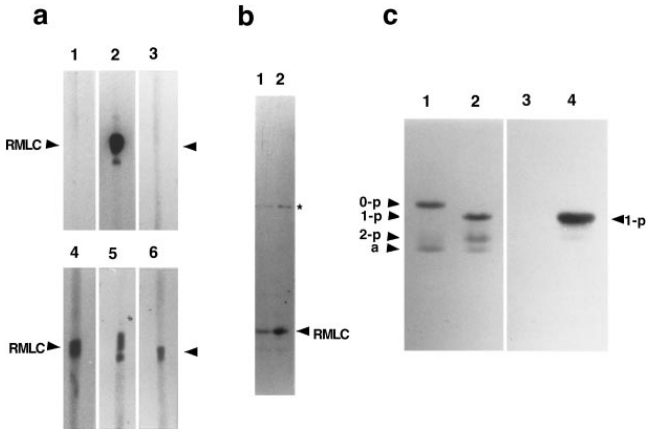

Figure 1. Specificity of pp2b antibody against S19-phosphorylated regulatory myosin light chain. (*a*) The pp2b antibody reacts only with RMLC phosphorylated by MLCK (lane *2*), but not with unphosphorylated RMLC (lane *1*) nor RMLC phosphorylated by protein kinase C (lane *3*). The identical samples of phosphorylated or unphosphorylated RMLC were separated by SDS-PAGE, transferred (lanes *1* and *4*, unphosphorylated RMLC; lanes *2* and *5*, RMLC phosphorylated by MLCK; lanes *3* and *6*, RMLC phosphorylated by PKC), and then immunoblotted with either pp2b (lanes *1–3*) or a monoclonal antibody against RMLC (lanes *4–6*). Note that pp2b reacted only with RMLC phosphorylated by MLCK (lane *2*), whereas the monoclonal antibody reacted with all kinds of RMLC (lanes *4–6*). (*b*) Immunoblot of total cell lysates with pp2b antibody. The antibody reacted with a band whose relative molecular mass corresponds to RMLC (*arrowhead*). Note that the reactivity was considerably increased when the phosphorylation of RMLC in the total cell lysates is increased in vitro by incubation with MLCK (lane *2*), confirming that the band is indeed phosphorylated RMLC. A band with an approximate molecular weight of 50,000 (*asterisk*) cross-reacted slightly with pp2b. The identity of the 50-kD band is currently unknown. (*c*) pp2b reacts predominantly with mono-phosphorylated RMLC. Urea/glycerol gel analyses were performed to separate unphosphorylated (*0-p*), mono-phosphorylated (*1-p*), di-phosphorylated (*2-p*), and myosin light chain–1 (*a*). Lanes *1* and *3*, unphosphorylated myosin light chains; lanes *2* and *4*, phosphorylated myosin light chains. Lanes *1* and *2* were stained with Coomassie blue, and lanes *3* and *4* were immunoreacted with pp2b. Note that pp2b reacted strongly with mono-phosphorylated (*1-p*), but not with unphosphorylated (*0-p*) RMLC. The reactivity to di-phosphorylated (*2-p*) RMLC was very weak.

Cell Culture and Indirect Double-Label Immunofluorescence

Cultured cells used include REF-52 cells (rat embryo derived fibroblastic cells), REF-2A cells (SV-40 transformed REF52 cells), gerbil fibroma cells (IMR-33; CCL146; American Type Culture Collection, Rockville, MD), and epithelial type NRK cells (NRK-52E, CRL1571, American Type Culture Collection). Cells were maintained in DME containing 10% new born calf serum.

Double-label immunofluorescence was performed as described before (34). Briefly, cells grown on glass coverslips were fixed with 3.7% formaldehyde solution in PBS, permeabilized with acetone at −20°C, and then incubated with primary antibodies of pp2b (60 μg/ml) and a mouse monoclonal antibody against heavy chain of myosin II (called monoclonal myosin antibody; Immunotech, Westbrook, ME). After extensive washing, cells were labeled with affinity-purified, rhodamine-conjugated goat anti–mouse, and FITC-conjugated goat anti–rabbit antibodies. The monoclonal myosin antibody was originally reported to react with platelet myosin (18, 21), indicating that it recognizes myosin IIA. We found however, that the monoclonal myosin antibody reacts with myosin IIB as well as myosin IIA. First, the monoclonal myosin antibody strongly stained myosin II in COS cells (which contain only myosin IIB). Second, the staining patterns of a variety of cells with this monoclonal myosin antibody are essentially the same as those stained with a mixture of antibodies against myosin IIA and myosin IIB (supplied by Dr. Itoh, Osaka Medical Center for Cancer and Cardiovascular Diseases, Osaka, Japan).

In some experiments, double-label immunofluorescence localization of S19-phosphorylated RMLC and myosin heavy chain was performed with pp2b and polyclonal rabbit antibodies against myosin heavy chain. This was performed by biotinylating either pp2b or rabbit antibodies. The polyclonal anti–heavy chain antibodies used are (*a*) an antibody against human platelet myosin heavy chain (called platelet myosin antibody; supplied by Drs. J. Sellers and R. Adelstein, NIH, Bethesda, MD), and (*b*) a mixture of polyclonal antibodies directed against myosin IIA and myosin IIB heavy chain (called myosin IIAB antibody). Whereas the platelet myosin antibody was originally raised against myosin IIA, we found that it also reacted, though the titer is somewhat lower, with myosin IIB (checked by staining of COS cells). Three combinations of antibodies were tested: platelet myosin antibody and biotinylated pp2b; pp2b and biotinylated platelet myosin antibody; and biotinylated pp2b and myosin IIAB antibody. Cells were first incubated with unbiotinylated antibody, and then labeled with rhodamine-conjugated goat anti–rabbit antibody. After extensive washing with PBS, the cells were incubated with an affinity-purified, unconjugated, rabbit antibody (1 mg/ml) to block all reactive sites of the goat anti–rabbit antibody. The cells were again washed with PBS, and then fixed for 5 min with 3.7% formaldehyde. After washing with PBS, the cells were incubated with biotinylated antibody. FITC-conjugated streptavidin was then used to detect the biotinylated antibody. We found that the results obtained with any of these combinations are similar to those obtained with the double labeling using pp2b and the monoclonal myosin antibody. Double-label localization of S19-phosphorylated RMLC and F-actin was performed as described (13).

Phase and fluorescence images were taken with an AT200 cooled CCD black and white camera (Photometric, Tucson, AZ) with Micro-Tome image processing software (VayTek, Fairfield, IA). Exposure time was adjusted to obtain rhodamine and FITC images with roughly equal intensities (checked by histogram analysis). Alignment of FITC and corresponding rhodamine images was made using 1 μm TetraSpeck fluorescent microspheres (Molecular Probes, Eugene, OR). Grayscale rhodamine and FITC images were converted into red and green images, respectively, and then merged to synthesize RGB color images. A ratio image of Fig. 3 (*E*) was created using an ImagePro image processing system. A grayscale image of pp2b staining was divided by a corresponding grayscale image of total myosin, and the resultant image was multiplied by 100. This operation yielded the image with the highest grayscale ~100 (which means a ratio value of 1). In some experiments, phase and immunofluorescence micrographs were taken using Kodak Technical Pan films (Rochester, NY) and T-Max P400 films (Kodak, Rochester, NY), respectively.

Results

Specificity of pp2b to S19-phosphorylated RMLC

The antibody (called pp2b) was raised by immunizing a

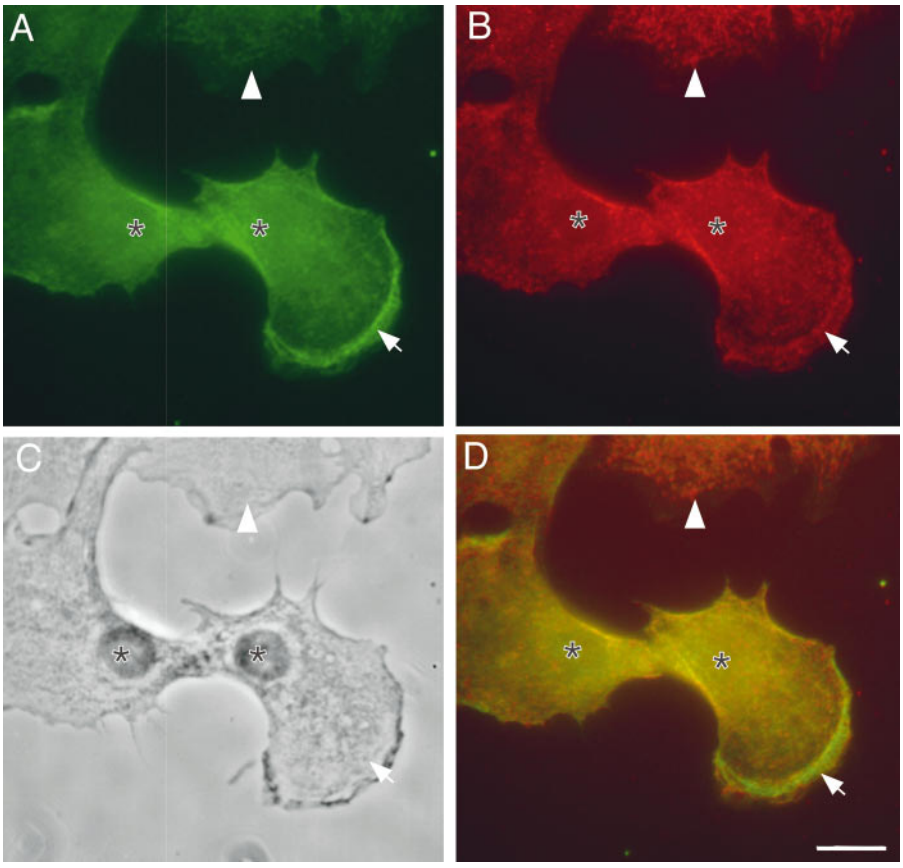

Figure 2. Localization of S19-phosphorylated myosin (P-myosin) in motile fibroblasts. Gerbil fibroma cells were double stained with pp2b and a monoclonal antibody against myosin heavy chain. *A* shows immunofluorescence with pp2b; *B* shows immunofluorescence with the monoclonal myosin antibody; *C* shows a phase contrast image; and *D* shows a merged image (*green*, pp2b; *red*, monoclonal anti–heavy chain antibody). Note that P-myosin is enriched in microfilament bundles near membrane ruffles (*arrow*). The anterior region containing a nucleus (*asterisk*) is greenish, indicating that P-myosin is also enriched in this region. The upper side of each figure contains a well spread, relatively nonmotile cell (*arrowhead*). This cell is less stained with pp2b than with the monoclonal myosin antibody, indicating that the level of phosphorylation is low in such cell (see Fig. 4). Bar, 10 μm.

rabbit with a 12-mer phosphopeptide containing phosphoserine at position 19 of RMLC. We have concluded, as judged by the following results, that the antibody is specific to S19-phosphorylated RMLC. First, pp2b reacted only with MLCK-phosphorylated (serine 19–phosphorylated) RMLC (Fig. 1 *a*, lane *2*), but not with dephosphorylated, or PKC phosphorylated (serine 1, 2, and threonine 9–phosphorylated) RMLC (Fig. 1 *a*, lanes *1* and *3*). Second, pp2b reacted specifically with phosphorylated RMLC when total cell lysates of NRK cells (epithelial type, ATCC1571 [American Type Culture Collection]) were immunoblotted with pp2b. As Fig. 1 *b* shows, an immunoblot of a total cell lysate with pp2b showed a band corresponding to the molecular weight of RMLC (Fig. 1 *b*, lane *1*, *arrowhead*). This band was confirmed as phosphorylated RMLC, because preincubation of a lysate with MLCK and calmodulin (which increases the level of RMLC phosphorylation) resulted in an increased immunoreactivity of the band (Fig. 1 *b*, lane *2*). Third, immunoblots of RMLC separated on urea/glycerol gels revealed that pp2b reacted very strongly with monophosphorylated RMLC (Fig. 1 *c*, lane *4*), and slightly with diphosphorylated, but not at all with unphosphorylated RMLC (Fig. 1 *c*, lane *3*).

It should be noted that the immunoblot of total cell lysates also showed a very minor band with an apparent relative molecular mass of 50,000 (Fig. 1 *b*, *asterisk*). To check whether the reactivity to this minor band is because of contamination with other antibodies, pp2b is further affinity purified using PVDF membranes to which phosphorylated RMLC was transferred after the separation by SDS-PAGE. Such affinity-purified antibody still reacts with the 50-kD minor band (data not shown), suggesting that pp2b may cross-react with this unidentified protein. Alternatively, this minor band might be an oligomer of phosphorylated RMLC because the reactivity to this band seems to be increased after phosphorylation of RMLC with MLCK (see Fig. 1 *b*, lane *2*).

Localization of S19-phosphorylated RMLC in Interphase Fibroblasts

We have first examined the subcellular distribution of my-

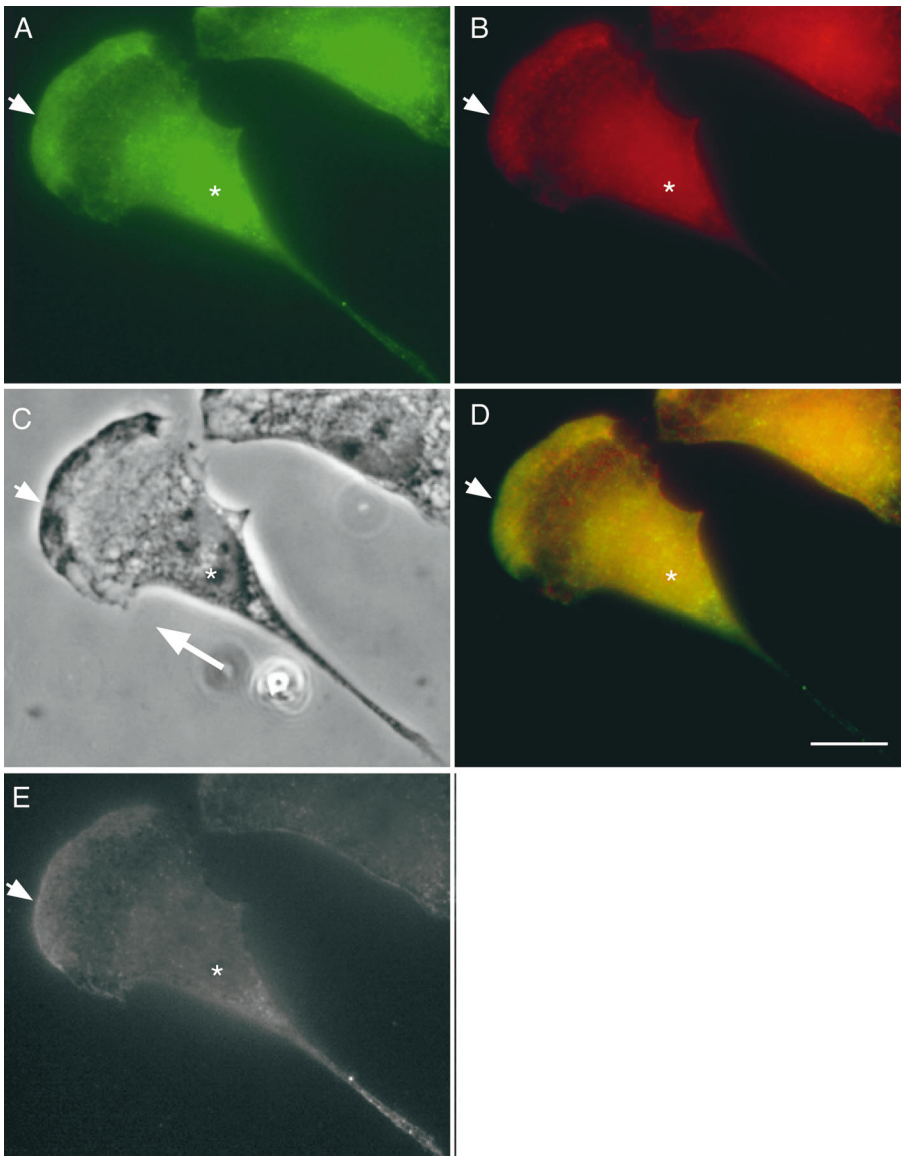

Figure 3. Bimodal distribution of P-myosin in a motile fibroblast of REF-2A. A motile REF-2A cell was double labeled with pp2b (*A*), and the monoclonal myosin antibody (*B*). (*C*) Phase contrast image. (*D*) Merged image (*green*, pp2b; *red*, anti–heavy chain antibody). (*E*) Ratio image of *A*/*B*. As shown in the merged image of *D*, both anterior (*arrowhead*) and posterior (the tail in particular) regions of the cell are greenish whereas the middle area is reddish, indicating that P-myosin is enriched in both anterior and posterior regions. The ratio image of *E* supports this notion. *Asterisk*, nucleus. A large white arrow in *C* shows the direction of cell locomotion. Bar, 10 μm.

osin phosphorylated at S19 (P-myosin) in motile fibroblasts. Fig. 2 shows the double-labeled immunolocalization of phosphorylated myosin (Fig. 2 *A*, *green*; detected by pp2b) and total myosin (Fig. 2 *B*, *red*; detected by the monoclonal myosin antibody) in motile gerbil fibroma cells with a polarized morphology. It appears that P-myosin (green) is enriched in microfilament bundles near membrane ruffles (Fig. 2 *A*, *arrow*). This enrichment becomes clear when these red and green images are merged (Fig. 2 *D*). The cell body containing the nucleus (Fig. 2 *D*, *asterisk*) seems also greenish, suggesting that the phosphorylation level of this region is increased.

The enrichment of P-myosin in both anterior and posterior regions is commonly observed with other motile fibroblasts with a polarized cell shape. Fig. 3 (*A–D*) shows the immunofluorescent images of P-myosin (green, stained with pp2b) and total myosin (red, stained with the monoclonal myosin antibody), a phase-contrast image, and a red/green merged image of REF-2A cells (an SV-40–transformed rat fibroblastic cell line), respectively. Again, the area close to membrane ruffles (Fig. 3, *arrow*), as well as the tail region (Fig. 3, *asterisk*) appears greenish, indicating that P-myosin is enriched in both regions. This bimodal distribution of P-myosin is observed in >80% of motile fibroblasts with a polarized morphology.

To further analyze the localization of P-myosin, a ratio image (Fig. 3 *E*) was generated by dividing the grayscale pattern of pp2b staining (Fig. 3 *A*) with the grayscale pattern of total myosin (Fig. 3 *B*). This analysis confirms that the motile fibroblast displays a roughly bimodal pattern of myosin phosphorylation along the direction of cell movement. The ratio is high at the front (where a cell shows membrane ruffles), and is then decreased to a low level in an area behind the membrane ruffles (though this area contains low levels of total myosin). The level of myosin phosphorylation is high again in a region of cell body containing the nucleus, and in particular the tail. This bimodal pattern of P-myosin suggests that cell motility of fibroblasts may require contraction at both posterior and anterior regions.

We have then examined the distribution of P-myosin in nonmotile fibroblasts with a well spread and nonpolarized morphology, and found that such cells exhibit distinct localization of P-myosin. First, as Fig. 4 shows, P-myosin is enriched in cortical actin filaments (Fig. 4, *arrow*) in such nonmotile cells. The staining with pp2b (Fig. 4 *A*; shown by green) is much stronger than that with the monoclonal myosin antibody (Fig. 4 *B*; shown by red). This is clearly seen when the red and green images are merged (Fig. 4 *C*). Second, P-myosin is enriched at cell periphery or membrane protrusions (Fig. 4, *arrowhead*). Third, nonmotile cells have in general a lower level of myosin phosphorylation than motile cells. This can be first recognized in Fig. 2, which contains such a cell at the upper side of each figure (Fig. 2, *arrowhead*). Although only a part of the cell is

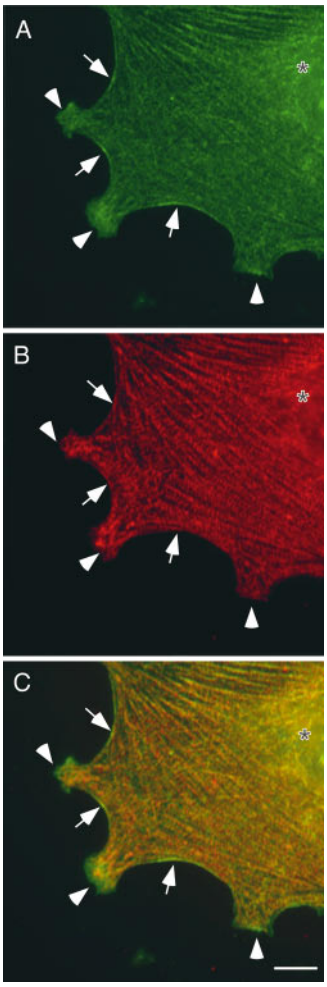

Figure 4. Localization of P-myosin in a fibroblast with a well-spread, nonpolarized morphology. A gerbil fibroma cell with well-developed stress fibers was double stained with pp2b (*A*) and the monoclonal myosin antibody (*B*). (*C*) A merged image (*green*, pp2b; *red*, the monoclonal myosin antibody). Note that cortical filaments (*arrow*) are stained more strongly with pp2b than with the monoclonal myosin antibody, indicating that P-myosin is enriched in cortical filaments. Membrane protrusions (*arrowhead*), as well as the area containing nucleus (*asterisk*) are also enriched with P-myosin. In contrast, stress fibers are red, indicating a lower level of myosin phosphorylation. Bar, 10 μm.

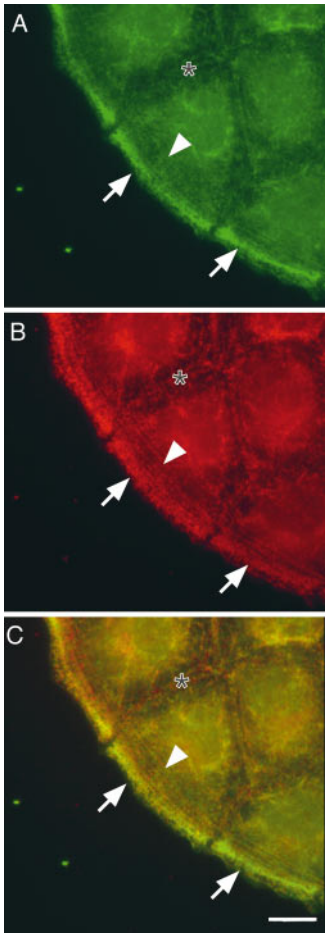

Figure 5. P-myosin is also enriched in peripheral microfilament bundles of a leading edge of a motile epithelial cell sheet. A motile epithelial cell sheet of NRK cells was double labeled with pp2b (*A*) and the monoclonal myosin antibody (*B*). (*C*) A merged image (*green*, pp2b; *red*, the monoclonal myosin antibody). Note that there is a discontinuous gradient of myosin phosphorylation; pp2b stains the microfilament bundles close to the cell periphery (*arrow*) more strongly than those present in an inner region of the cell (*arrowhead*). Also note that circumferential microfilament bundles adjacent to cell–cell contacts (*asterisk*) was less stained with pp2b than with the monoclonal myosin antibody. The merged image of *C* clearly shows that the most peripheral microfilament bundles are greenish whereas the circumferential bundles are reddish. Bar, 10 μm.

shown, the staining with pp2b (Fig. 2 *A*) is much weaker than that with the monoclonal myosin antibody (Fig. 2 *B*). The low level of phosphorylation is clearly indicated by a reddish stress fiber–like structure of this cell in the red/green merged image (Fig. 2 *D*). Fig. 4 confirms this. The stress fibers of this flat, nonmotile gerbil fibroma cell contains a lower level of P-myosin, which is evidenced by the red color of the merged image (Fig. 4 *C*). It should be noted that the area containing the nucleus is greenish, again indicating that the cell body appears to contain a higher level of P-myosin, just like motile fibroblasts.

Localization of P-myosin in Interphase Epithelial Cells

The enrichment of P-myosin in the cell periphery of motile fibroblasts is shared by epithelial cells forming a motile cell sheet. Fig. 5 shows localization of P-myosin (Fig. 5 *A*; pp2b), and total myosin (Fig. 5 *B*; monoclonal myosin antibody) of interphase NRK cells at the leading edge of an epithelial cell sheet. The differential distribution of P-myosin is again clearly seen in an image (Fig. 5 *C*) synthesized with the patterns of P-myosin (Fig. 5 *A*, *green*) and total myosin (Fig. 5 *B*, *red*). P-myosin is enriched in peripheral microfilament bundles immediately interior to membrane ruffles of the leading edge (arrow in Fig. 5, *A–C*; less peripheral microfilaments are indicated by an *arrowhead*). There appears to be a gradient of S19 phosphorylation even within the layers of these peripheral microfilament bundles, with those closer to the leading edge more distinctly stained with pp2b. Notably, circumferential microfilament bundles near cell–cell contacts were not stained with pp2b (Fig. 5, *A–C*, *asterisk*), suggesting that myosin in such bundles may have a structural function, rather than a contractile one.

We have then examined the localization of P-myosin during wound healing. Fig. 6 shows the localization of P-myosin (Fig. 6 *A*; pp2b) and total myosin (Fig. 6 *B*; monoclonal myosin antibody) in a wound which is partially closing. A merged image (*green*, pp2b; *red*, monoclonal myosin antibody) synthesized with the above two localization patterns reveals that P-myosin is enriched in the cell periphery as well as the region of closing (*arrowhead*).

Finally, we examined the regulation of S19 phosphorylation during the other type of coordinated cell movement, i.e., the closing of a small cell-free opening surrounded by an epithelial cell sheet. Unlike cells during wound healing, NRK cells surrounding the opening show no membrane ruffles at the edge of the opening. Fig. 7 (*A* and *B*) shows the localization of P-myosin (detected by pp2b) and total myosin (detected by platelet myosin antibody), respectively. Phosphorylated myosin was clearly localized in the microfilament bundles surrounding the ring or arc at the border of the opening (Fig. 7, *arrows*). A red/green merged image (Fig. 7 *C*) demonstrates that the ring is yellow, reflecting an enrichment of both phosphorylated and unphosphorylated myosin. This observation indicates that

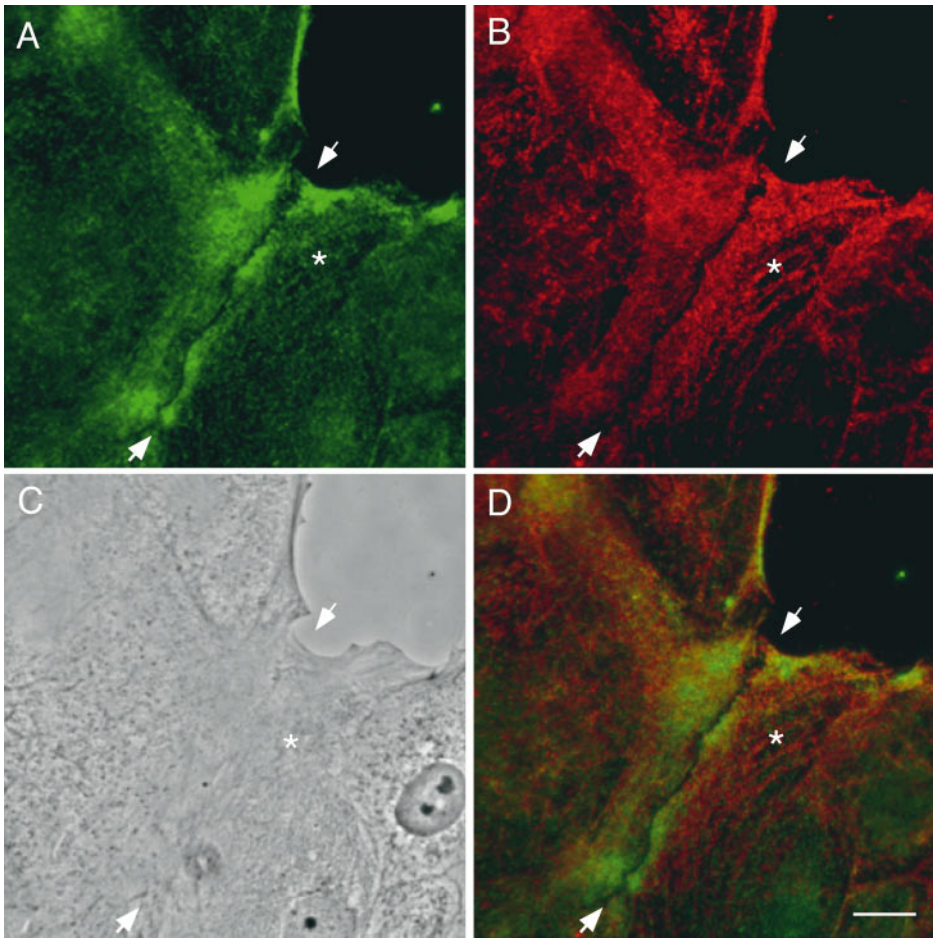

Figure 6. Localization of P-myosin during wound closing of epithelial cells. NRK cells were stained with pp2b (*A*) and the monoclonal myosin antibody (*B*). (*C*) Phase contrast. (*D*) Merged image (*green*, pp2b; *red*, the monoclonal myosin antibody). pp2b stains the region of closing (*arrowhead*) more strongly than the microfilament bundles in an inner region (*asterisk*), again indicating a discontinuous gradient of myosin phosphorylation. Bar, 10 μm.

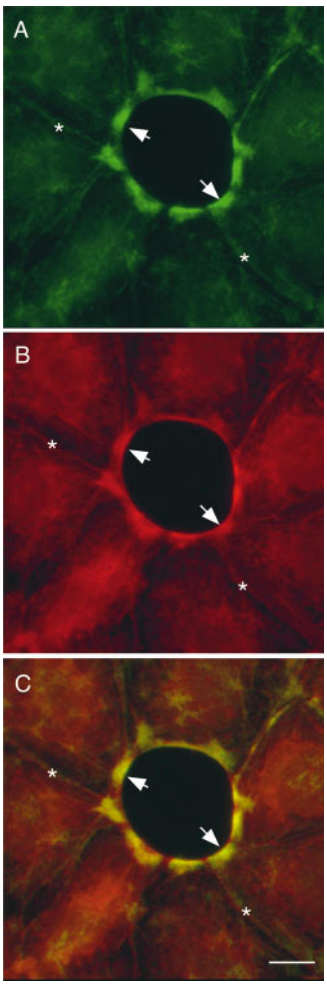

Figure 7. Specific localization of P-myosin at a small opening of an epithelial sheet. (*A*) Staining with pp2b. (*B*) Staining with the biotinylated platelet myosin antibody. (*C*) A merged image (*green*, pp2b; *red*, platelet myosin antibody). Note that the ring or arc surrounding the opening (*arrow*) was strongly stained with pp2b, suggesting that myosin phosphorylation and contraction are required for the closure of an opening. The pp2b staining of circumferential actin bundles adjacent to cell–cell contacts (*asterisk*) is much weaker than is the staining with the anti–heavy chain antibody, indicating that phosphorylated myosin is not enriched in these circumferential actin bundles. Bar, 10 μm.

the ring was contracting to close the small hole, consistent with the "purse-string" model for small wound closure (2). On the other hand, the circumferential actin bands (Fig. 7, *asterisks*) are reddish, again indicating a low level of myosin phosphorylation.

Localization of S19-phosphorylated RMLC in Dividing Cells

To study when and where S19 phosphorylation occurs during mitosis of epithelial cells, NRK cells at different mitotic stages were examined by immunostaining with pp2b and counterstaining with the platelet myosin antibody. Fig. 8, *D–F* shows a prophase cell (*right*), whereas a metaphase cell is shown in Fig. 8, *A–C*. From prophase to metaphase, pp2b only stains the spindle poles (e.g., Fig. 8 *B*, *arrowhead*). Consistent with previous reports (9, 27), the antibody against heavy chain does not reveal any filamentous structures in these cells (Fig. 8, *C* and *F*). The significance of the pp2b staining of spindle poles is unclear. However, the observation suggests that myosin IIA may be phosphorylated here at the spindle pole because similar staining is observed with the antibody against heavy chain of myosin IIA (15). Alternatively, it may be that centrioles contain the unknown cross-reactive protein of about 50 kD seen in western blots probed with pp2b (Fig. 1 *b*).

In late anaphase (Fig. 8, *D–F*, *left*), pp2b stains the midzone between the separating chromosomes (Fig. 8 *E*, *arrowhead*), a staining pattern that is also seen with the antibody against heavy chain (Fig. 8 *F*, *arrowhead*). The timing of pp2b staining in the midzone seems to be precisely controlled; staining is observed only at late stages of anaphase, but is never observed before chromatid separation or during early stages of chromosome separation (early anaphase). This staining precedes the formation of a cleavage furrow and appears to reach beyond the mitotic spindles, stopping short of the peripheral region where the cleavage furrow would later form. In telophase (Fig. 8, *G–I*), pp2b staining is seen at the cleavage furrows, where it persists until the end of cytokinesis. It should be noted that pp2b staining patterns in a cleavage furrow are, for the most part, coincidental with those obtained with the antibody against heavy chain. This indicates that myosin filaments forming a cleavage furrow are phosphorylated, and that this filament assembly and phosphorylation occur at approximately the same time. This observation is consistent with the in vitro finding that S19 phosphorylation of RMLC favors the assembly of myosin filaments.

We also examined whether the assembly of F-actin shows any correlation with the appearance of P-myosin in the midzone between the separating chromosomes during late anaphase. Fig. 9, *A* and *B*, shows the localization of P-myosin and F-actin, respectively, in the very beginning of late anaphase when P-myosin starts to accumulate. F-actin appears to colocalize with P-myosin as soon as pp2b staining of the interchromosomal midzone (Fig. 9, *arrowhead*) is seen. Taken together with the above observation that P-myosin colocalized with total myosin in dividing cells, these findings suggest that S19 phosphorylation occurs simultaneously with the assembly of actin and myosin.

Fig. 10 shows color images of dividing REF-2A cells (Fig. 10, *A*) and NRK epithelial cells (Fig. 10, *C*), where green and red indicate the localization of P-myosin (detected by pp2b) and total myosin (detected by the monoclonal myosin antibody), respectively. Fig. 10 *A* shows two mitotic fibroblasts, one in metaphase and the other in telophase. Whereas the anaphase cell is red, the telophase cell is yellow, indicating that phosphorylation clearly occurs during cytokinesis. In addition, it is clear, as judged by the yellow color, that a contractile ring (Fig. 10, *arrow*) is stained with both pp2b and the antibody against heavy chain. Fig. 10 *C* demonstrates that the cleavage furrow of the dividing epithelial cell is greenish yellow, again indicating an enrichment of both phosphorylated and unphosphorylated myosin. In addition, the entire cell is slightly greenish and is surrounded by red interphase cells, indicating that the myosin phosphorylation level is higher in the cell at telophase. These observations are consistent with our previous biochemical study that S19 phosphorylation occurs during cytokinesis (33). Overall, our observations suggest that S19 phosphorylation of RMLC constitutes one of the critical steps leading to the formation and activation of contractile rings for cytokinesis.

Discussion

Specificity of pp2b

Our pp2b antibody is highly specific to S19 mono-phos-

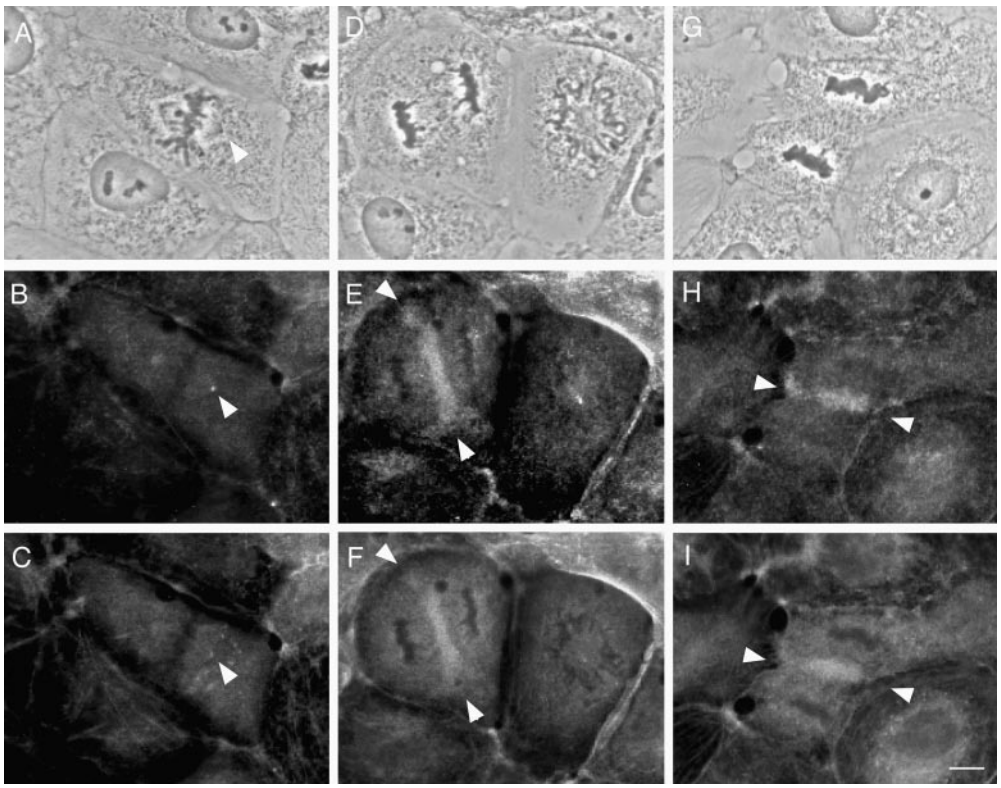

Figure 8. Immunolocalization of phosphorylated myosin in NRK cells at different mitotic stages. *Top*, phase-contrast; *middle*, stained with pp2b; *bottom*, stained with the biotinylated platelet myosin antibody. (*A–C*) Metaphase. Only spindle poles stained strongly (*arrowhead*). (*D–F*) Anaphase cell on the left. The midzone between the separating chromosomes was strongly stained (*arrowhead*). The neighboring cell was at prophase and only spindle pole staining was observed. (*G–I*) Telophase. A cleavage furrow (*arrowhead*) was strongly stained. Bar, 10 μm.

phorylated RMLC. It is thus possible that the localization of di-phosphorylated RMLC is not reflected in pp2b staining patterns. However, we believe, for the following reason, that the pp2b staining patterns include the localization of both mono- and di-phosphorylated RMLC. Di-phosphorylation of RMLC at T18 occurs only after mono-phosphorylation at S19. In addition, the content of di-phosphorylated RMLC is rather low; for example, virtually no di-phosphorylated myosin is detected in interphase REF-4A cells, and even during cytokinesis, <10% of total myosin is di-phosphorylated myosin (33). It is thus likely that myosin filaments, if they contain di-phosphorylated species of myosin, should carry mono-phosphorylated myosin as well. In fact, when myosin filaments are formed in vitro with a 1:1 mixture of mono- and di-phosphorylated myosin, pp2b stains all myosin filaments (data not shown), indicating that both mono- and di-phosphorylated myosin copolymerize. It is thus reasonable to assume that pp2b staining patterns represent the localization of both mono- and di-phosphorylated species of myosin.

Enrichment of Myosin Phosphorylation at Both Leading Edge and Tail of Motile Fibroblasts

Our antibody localization demonstrated that motile fibroblasts exhibit a bimodal distribution of P-myosin along the direction of cell movement; phosphorylation is high both at leading edge and tail of motile fibroblasts. This is a new finding. Whereas the high myosin phosphorylation in the tail is consistent with the previous result obtained by the biosensor method (25), phosphorylation at the leading edge has not been detected. The reason for this discrepancy is not known at this time. In a more recent study using the same method, however, P-myosin is sometimes detected in a leading edge during postmitotic cell spreading (6).

Phosphorylation at the tail is likely to be responsible for pushing a cell body forward by tail contraction. It may also function to transport actomyosin filaments to the leading edge. What is the function of myosin phosphorylation at the leading edge? There are at least two possibilities. First, the contractile activity of myosin II may contribute to the membrane extensions at the leading edges, although actin polymerization appears to be a major driving force for membrane protrusions (5, 32). For example, local contraction through myosin phosphorylation may alter cortical tension at this region of membrane, thereby helping the extension of membranes. Alternatively, it is possible that myosin II may help translocation of actin filaments at the leading edge, just as myosin I has been proposed to do (5, 32). The second possibility is that myosin phosphorylation at this region would be required for maintenance of polarized cell shape at the leading edge, counteracting the expanding force exerted by tail contraction. In any case, myosin phosphorylation at the leading edge is likely to play a critical role in cell locomotion because we have seen similar enrichment of P-myosin in a leading edge of a motile epithelial cell sheet.

Myosin Phosphorylation of Peripheral Microfilament Bundles in Motile Epithelial Cells

We have observed that (*a*) P-myosin is concentrated in peripheral microfilament bundles interior to the membrane ruffles of the leading edge of a motile epithelial sheet during wound healing; (*b*) P-myosin forms a "ring" or "arc" at the border of a small cell-free opening of an epithelial cell

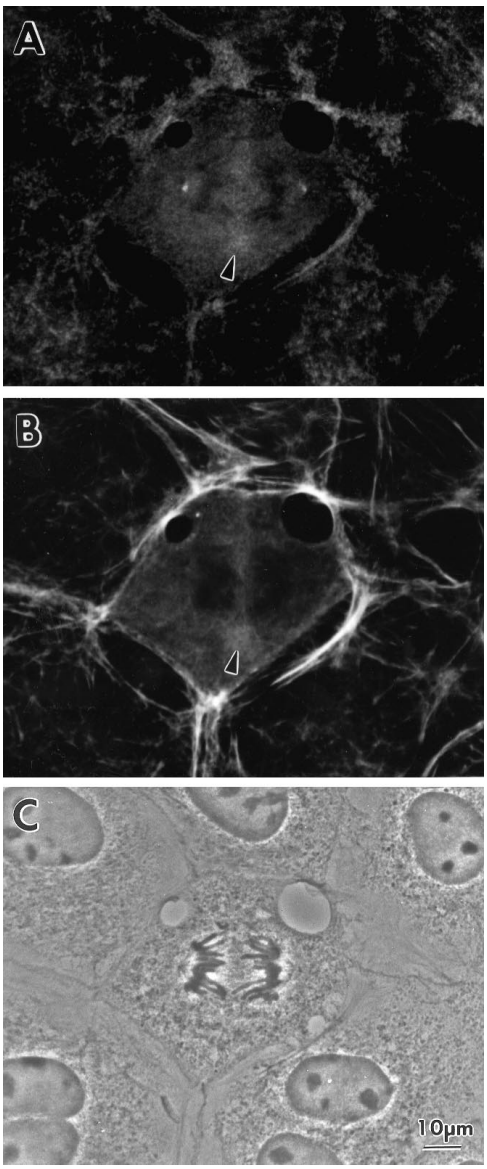

Figure 9. Simultaneous localization of phosphorylated myosin and F-actin in a mitotic cell at the beginning of late anaphase. (*A*) Stained with pp2b. (*B*) Stained with rhodamine phalloidin. (*C*) A phase contrast image. Note that actin accumulation occurs at approximately the same time as phosphorylated myosin appears.

sheet; and (*c*) P-myosin is not concentrated in circumferential microfilament bundles near cell–cell contacts.

The high level of myosin phosphorylation in the peripheral microfilament bundles indicates that this region of actomyosin is contractile, in contrast to the actomyosin present in circumferential microfilament bundles near cell–cell contacts. As discussed above in the case of fibroblasts, the contractility of the peripheral microfilament bundles may be required to produce the force needed to drive cell margins forward, or alternatively, the tension produced by the peripheral bundles may be needed to maintain the morphology of the leading edge of an epithelial sheet.

There is clearly a discontinuous gradient of P-myosin in peripheral microfilament bundles in a motile epithelial sheet. The exact mechanisms regulating the restriction of S19 phosphorylation to the periphery of these epithelial cells are unknown. This precise control of phosphorylation and dephosphorylation within a narrow region of the cell periphery may be affected by a gradient of a second messenger (e.g., calmodulin or Ca^{2+}) that regulates the activity of MLCK, or by a gradient of a kinase or phosphatase. Whatever the controlling factors, the ability to visualize this subcellular localization of myosin phosphorylation provides a novel approach to analyzing the precise regulation of cell movements during wound healing and morphogenesis. We are particularly interested in applying this technique to study the pattern of myosin phosphorylation in cell monolayers mediating embryonic morphogenesis, such as those involved in the closure of the dorsal lip of the blastopore.

Localization of Phosphorylated Myosin in Dividing Cells

Myosin II phosphorylation is precisely regulated, both spatially and temporally, in dividing cells. In both epithelial and fibroblastic cells, we have observed that a phosphorylation level increases upon cytokinesis (Fig. 10). This confirms our previous biochemical work, where an increase in S19 phosphorylation is observed when a majority of cells undergo cytokinesis (33).

A relatively flat morphology of the rat epithelial cells during mitosis has allowed us to make the following observations: (*a*) P-myosin appears in the midzone of the separating chromosomes during late anaphase but not before chromatin separation or early anaphase; (*b*) phosphorylation of myosin occurs before the formation of cleavage furrows; (*c*) P-myosin is concentrated at cleavage furrows until the end of cytokinesis; and (*d*) phosphorylation of myosin occurs at approximately the same time as the assembly of myosin and F-actin.

These observations, together with our previous biochemical data (33), indicate that myosin phosphorylation immediately precedes the formation of cleavage furrows, which is consistent with the report using the biosensor method (6). The nature of the signals resulting in the activation of a kinase(s) or the deactivation of a phosphatase (either or both of which would be required to produce the observed changes in RMLC phosphorylation) remain to be determined. Ca^{2+} is probably involved, since transient or continuous elevations of Ca^{2+} levels have been reported to precede or coincide with cytokinesis (4, 8), and MLCK requires Ca^{2+} and calmodulin for its activity (28). A recent report has suggested the involvement of myosin light chain phosphatase and RhoA (16); RhoA plays a role in completion of cytokinesis (17, 22). Rho kinase activated by GTP-bound RhoA has been shown to phosphorylate the myosin binding subunit of myosin light chain phosphatase, resulting in the inhibition of myosin light chain phosphatase. This inhibition of myosin light chain phosphatase may be involved in the phosphorylation of RMLC during cytokinesis. More recently, the same group has shown that Rho kinase can directly phosphorylate RMLC and suggested that this kinase may be responsible for cytokinesis (1, 20).

The ability to visualize the S19 phosphorylation of myosin II provides a new tool for the dissection of the subcellu-

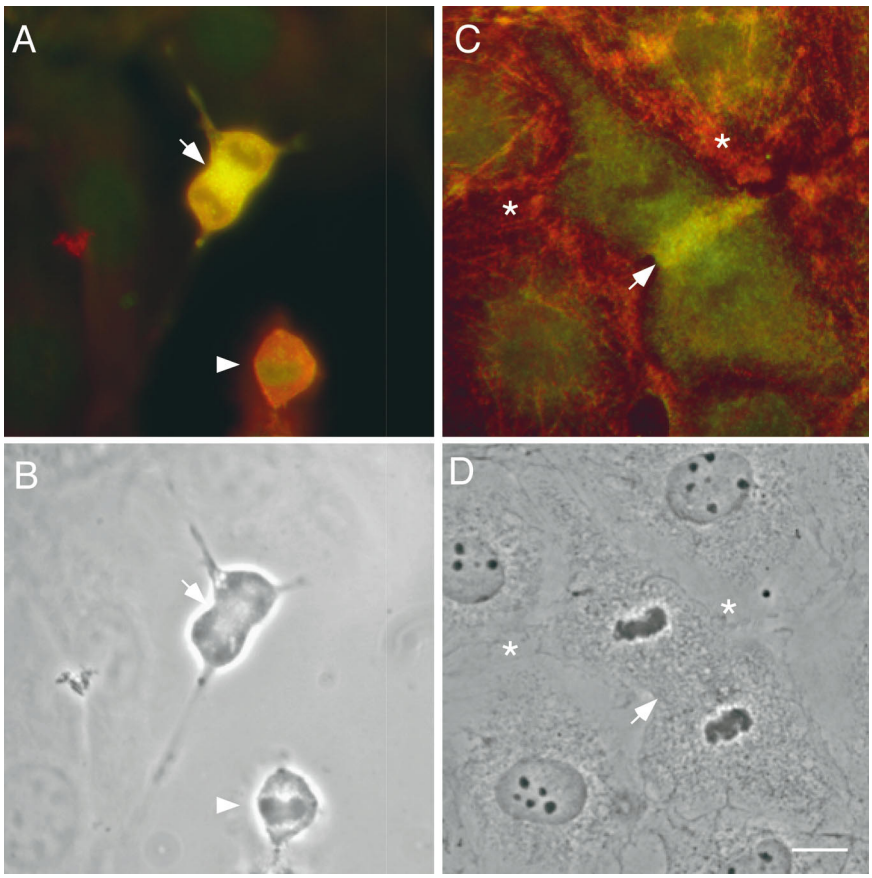

Figure 10. Localization of P-myosin in dividing cells. Dividing REF-2A (*A*) and NRK epithelial (*C*) cells were double stained with pp2b and the monoclonal myosin antibody and color images are synthesized (*green*, pp2b; *red*, monoclonal myosin antibody). B and D, corresponding phase-contrast images. A, phosphorylated myosin is enriched in a cleavage furrow of an REF-2A cell at telophase (*arrow*). On the other hand, a cell at metaphase (*arrowhead*) is red, indicating that the phosphorylation level is low during metaphase. (*C*) Phosphorylated myosin is enriched in a cleavage furrow (*arrow*) of a dividing NRK cell. Note that stress fibers as well as circumferential bundles of surrounding cells are reddish, indicating that the phosphorylation level is low with these structures. Bar, 10 μm.

lar events that orchestrate the internal and external movements of cells and tissues. The use of this new tool has allowed us to confirm and extend biochemical studies suggesting the importance of this specific phosphorylation event. The tool has both an advantage and a disadvantage in comparison to the method using the fluorescent biosensor (6, 25). The advantage is that the localization with the antibody seems to show better resolution than the biosensor method (it also does not require a sophisticated imaging system). The biosensor method has an advantage in that it can show dynamic behavior of P-myosin in living cells. On the other hand, the antibody localization requires fixation. These two independent methods should complement each other and will allow us to further characterize the precise factors responsible for effecting and controlling the phosphorylation of this particular amino acid residue of this key contractile protein.

We thank Drs. J. Sellers and R. Adelstein for their gift of anti-platelet myosin antibody; Dr. K. Itoh for his gift of anti–myosin IIA and IIB antibody. We also thank Dr. F. Deis (Rutgers University) for critical reading of this manuscript.

This work was supported by a grant (CA42742) from National Institutes of Health. F. Matsumura is a member of the Cancer Institute of New Jersey.

Received for publication 2 October 1997 and in revised form 6 November 1997.

References

1. Amano, M., M. Ito, K. Kimura, Y. Fukata, K. Chihara, T. Nakano, Y. Matsuura, and K. Kaibuchi. 1996. Phosphorylation and activation of myosin by Rho-associated kinase (Rho-kinase). *J. Biol. Chem.* 271:20246–20249.
2. Bement, W.M., P. Forscher, and M.S. Mooseker. 1993. A novel cytoskeletal structure involved in purse string closure and cell polarity maintenance. *J. Cell Biol.* 121:565–578.
3. Bennett, J.P., R.A. Cross, J. Kendrick-Jones, and A.G. Weeds. 1988. Spatial pattern of myosin phosphorylation in contracting smooth muscle cells: Evidence for contractile zones. *J. Cell Biol.* 107:2623–2629.
4. Chang, D.C., and C. Meng. 1995. A localized elevation of cytosolic free calcium is associated with cytokinesis in the zebrafish embryo. *J. Cell Biol.* 131:1539–1545.
5. Cramer, L.P., T.J. Mitchison, and J.A. Theriot. 1994. Actin-dependent motile forces and cell motility. *Curr. Opin. Cell Biol.* 6:82–86.
6. DeBiasio, R.L., G.M. LaRocca, P.L. Post, and D.L. Taylor. 1996. Myosin II transport, organization, and phosphorylation: evidence for cortical flow/solation-contraction coupling during cytokinesis and cell locomotion. *Mol. Biol. Cell.* 7:1259–1282.
7. Egelhoff, T.T., R.J. Lee, and J.A. Spudich. 1993. Dictyostelium myosin heavy chain phosphorylation sites regulate myosin filament assembly and localization in vivo. *Cell.* 75:363–371.
8. Fluck, R.A., A.L. Miller, and L.F. Jaffe. 1991. Slow calcium waves accompany cytokinesis in *medaka* fish eggs. *J. Cell Biol.* 115:1259–1265.
9. Fujiwara, K., and T.D. Pollard. 1976. Fluorescent antibody localization of myosin in the cytoplasm, cleavage furrow and mitotic spindle of human cells. *J. Cell Biol.* 71:848–875.
10. Giuliano, K.A., J. Kolega, R.L. DeBiasio, and D.L. Taylor. 1992. Myosin II phosphorylation and the dynamics of stress fibers in serum-deprived and stimulated fibroblasts. *Mol. Biol. Cell.* 3:1037–1048.
11. Goeckeleer, M.Z., and R.B. Wysolmerski. 1995. Myosin light chain kinase–regulated endothelial cell contraction: The relationship between isometric tension, actin polymerization, and myosin phosphorylation. *J. Cell Biol.* 130:613–627.
12. Hammer, J.A. 1994. Regulation of Dictyostelium myosin II by phosphorylation: what is essential and what is important? *J. Cell Biol.* 127:1779–1782.
13. Hosoya, N., H. Hosoya, S. Yamashiro, H. Mohri, and F. Matsumura. 1993. Localization of caldesmon and its dephosphorylation during cell division. *J. Cell Biol.* 121:1075–1082.
14. Kamm, K.E., and J.T. Stull. 1985. The function of myosin and myosin light chain kinase phosphorylation in smooth muscle. *Annu. Rev. Pharmacol. Toxicol.* 25:593–620.

15. Kelley, C.A., J.R. Sellers, D.L. Gard, D. Bui, R.S. Adelstein, and I.C. Baines. 1996. Xenopus nonmuscle myosin heavy chain isoforms have different subcellular localizations and enzymatic activities. *J. Cell Biol.* 134: 675–687.
16. Kimura, K., M. Ito, M. Amano, K. Chihara, Y. Fukata, M. Nakafuku, B. Yamamori, J. Feng, T. Nakano, K. Okawa, et al. 1996. Regulation of myosin phosphatase by Rho and Rho-associated kinase (Rho-kinase). *Science.* 273:245–248.
17. Kishi, K., T. Sasaki, S. Kuroda, T. Itoh, and Y. Takai. 1993. Regulation of cytoplasmic division of Xenopus embryo by rho p21 and its inhibitory GDP/GTP exchange protein (rho GDI). *J. Cell Biol.* 120:1187–1195.
18. Klotz, C., N. Bordes, M.C. Laine, D. Sandoz, and M. Bornens. 1986. Myosin at the apical pole of ciliated epithelial cells as revealed by a monoclonal antibody. *J. Cell Biol.* 103:613–619.
19. Kolodney, M.S., and E.L. Elson. 1993. Correlation of myosin light chain phosphorylation with isometric contraction of fibroblasts. *J. Biol. Chem.* 268:23850–23855.
20. Kureishi, Y., S. Kobayashi, M. Amano, K. Kimura, H. Kanaide, T. Nakano, K. Kaibuchi, and M. Ito. 1997. Rho-associated kinase directly induces smooth muscle contraction through myosin light chain phosphorylation. *J. Biol. Chem.* 272:12257–12260.
21. Lemullois, M., C. Klotz, and D. Sandoz. 1987. Immunocytochemical localization of myosin during ciliogenesis of quail oviduct. *Eur. J. Cell Biol.* 43:429–437.
22. Mabuchi, I., Y. Hamaguchi, H. Fujimoto, N. Morii, M. Mishima, and S. Narumiya. 1993. A rho-like protein is involved in the organisation of the contractile ring in dividing sand dollar eggs. *Zygote.* 1:325–331.
23. Ostrow, B.D., P. Chen, and R.L. Chisholm. 1994. Expression of a myosin regulatory light chain phosphorylation site mutant complements the cytokinesis and developmental defects of *Dictyostelium* RMLC null cells. *J. Cell Biol.* 127:1945–1955.
24. Perrie, W.T., and S.V. Perry. 1970. An electrophoretic study of the low-molecular-weight components of myosin. *Biochem J.* 119:31–38.
25. Post, P.L., R.L. DeBiasio, and D.L. Taylor. 1995. A fluorescent protein biosensor of myosin II regulatory light chain phosphorylation reports a gradient of phosphorylated myosin II in migrating cells. *Mol. Biol. Cell.* 6:1755–1768.
26. Sakurada, K., T. Ikuhara, M. Seto, and Y. Sasaki. 1994. An antibody for phosphorylated myosin light chain of smooth muscle: application to a biochemical study. *J. Biochem. (Tokyo).* 115:18–21.
27. Sanger, J.M., B. Mittal, J.S. Dome, and J.W. Sanger. 1989. Analysis of cell division using fluorescently labeled actin and myosin in living PtK2 cells. *Cell Motil. Cytoskeleton.* 14:201–219.
28. Sellers, J.R. 1991. Regulation of cytoplasmic and smooth muscle myosin. *Curr. Opin. Cell Biol.* 3:98–104.
29. Spudich, J.A. 1989. In pursuit of myosin function. *Cell Regul.* 1:1–11.
30. Trybus, K.M. 1991. Regulation of smooth muscle myosin. *Cell Motil. Cytoskeleton.* 18:81–85.
31. Uyeda, T.Q., and J.A. Spudich. 1993. A functional recombinant myosin II lacking a regulatory light chain-binding site. *Science.* 262:1867–1870.
32. Welch, M.D., A. Mallavarapu, J. Rosenblatt, and T.J. Mitchison. 1997. Actin dynamics in vivo. *Curr. Opin. Cell Biol.* 9:54–61.
33. Yamakita, Y., S. Yamashiro, and F. Matsumura. 1994. In vivo phosphorylation of regulatory light chain of myosin II during mitosis of cultured cells. *J. Cell Biol.* 124:129–137.
34. Yamashiro-Matsumura, S., and F. Matsumura. 1986. Intracellular localization of the 55-kD actin-bundling protein in cultured cells: spatial relationships with actin, alpha-actinin, tropomyosin, and fimbrin. *J. Cell Biol.* 103:631–640.
35. Yumura, S., and T.Q. Uyeda. 1997. Myosin II can be localized to the cleavage furrow and to the posterior region of *Dictyostelium* amoebae without control by phosphorylation of myosin heavy and light chains. *Cell Motil. Cytoskeleton.* 36:313–322.